JOURNAL OF THE AMERICAN COLLEGE OF CARDIOLOGY VOL. 66, NO. 1, 2015

ISSN 0735-1097/$36.00
PUBLISHED BY ELSEVIER INC. http://dx.doi.org/10.1016/j.jacc.2015.04.056

Atrial Fibrillation Activates AMP-Dependent Protein Kinase and its Regulation of Cellular Calcium Handling

Potential Role in Metabolic Adaptation and Prevention of Progression

Masahide Harada, MD, PhD,*† Artavazd Tadevosyan, MSc,* Xiaoyan Qi, PhD,* Jiening Xiao, PhD,* Tao Liu, PhD,*‡ Niels Voigt, MD,§ Matthias Karck, MD,‖ Markus Kamler, MD,¶ Itsuo Kodama, MD, PhD,# Toyoaki Murohara, MD, PhD,** Dobromir Dobrev, MD,§ Stanley Nattel, MD*

ABSTRACT

BACKGROUND Atrial fibrillation (AF) is associated with metabolic stress, which activates adenosine monophosphate-regulated protein kinase (AMPK).

OBJECTIVES This study sought to examine AMPK response to AF and associated metabolic stress, along with consequences for atrial cardiomyocyte Ca^{2+} handling.

METHODS Calcium ion (Ca^{2+}) transients (CaTs) and cell shortening (CS) were measured in dog and human atrial cardiomyocytes. AMPK phosphorylation and AMPK association with Ca^{2+}-handling proteins were evaluated by immunoblotting and immunoprecipitation.

RESULTS CaT amplitude and CS decreased at 4-min glycolysis inhibition (GI) but returned to baseline at 8 min, suggesting cellular adaptation to metabolic stress, potentially due to AMPK activation. GI increased AMPK-activating phosphorylation, and an AMPK inhibitor, compound C (CompC), abolished the adaptation of CaT and CS to GI. The AMPK activator 5-aminoimidazole-4-carboxamide ribonucleotide (AICAR) increased CaT amplitude and CS, restoring CompC-induced CaT and CS decreases. CompC decreased L-type calcium channel current ($I_{Ca,L}$), along with $I_{Ca,L}$-triggered CaT amplitude and sarcoplasmic reticulum (SR) Ca^{2+} content under voltage clamp conditions in dog cells and suppressed CaT and $I_{Ca,L}$ in human cardiomyocytes. Small interfering ribonucleic acid-based AMPK knockdown decreased CaT amplitude in neonatal rat cardiomyocytes. L-type Ca^{2+} channel α subunits coimmunoprecipitated with AMPKα. Atrial AMPK-activating phosphorylation was enhanced by 1 week of electrically maintained AF in dogs; fractional AMPK phosphorylation was increased in paroxysmal AF and reduced in longstanding persistent AF patients.

CONCLUSIONS AMPK is activated by metabolic stress and AF, and helps maintain the intactness of atrial $I_{Ca,L}$, Ca^{2+} handling, and cell contractility. AMPK contributes to the atrial compensatory response to AF-related metabolic stress; AF-related metabolic responses may be an interesting new therapeutic target. (J Am Coll Cardiol 2015;66:47–58)

From the *Department of Medicine and Research Center, Montreal Heart Institute and Université de Montréal, Montreal, Quebec, Canada; †Department of Cardiology, Fujita Health University School of Medicine, Toyoake, Japan; ‡Department of Cardiology, Renmin Hospital of Wuhan University, Wuhan, China; §Institute of Pharmacology, West German Cardiac and Vascular Center, School of Medicine, University Duisburg-Essen, Essen, Germany; ‖Department of Cardiac Surgery, Heidelberg University, Heidelberg, Germany; ¶Department of Cardiac Surgery, Huttrop Heart Center, Essen, Germany; #Nagoya University, Nagoya, Japan; and the **Department of Cardiology, Nagoya University Graduate School of Medicine, Nagoya, Japan. Dr. Nattel is supported by European-North American Atrial Fibrillation Research Alliance Fondation Leducq grant 07CVD03, Canadian Institutes of Health Research (44365), and Quebec Heart and Stroke Foundation. Dr. Harada is supported by Japanese Heart Rhythm Society/Medtronic fellowship and Japan Heart Foundation/Japanese Society of Electrocardiology scholarship. Dr. Tadevosyan is supported by Fonds de Recherche de Quebec en Santé-Réseau en Santé Cardiovasculaire/Heart and Stroke Foundation of Quebec

ABBREVIATIONS AND ACRONYMS

AMPK = adenosine monophosphate-activated protein kinase

Ca^{2+} = calcium ion

CaT = calcium ion transient

CompC = compound C

CS = cell shortening

GI = glycolysis inhibition

HPLC = high-performance liquid chromatography

$I_{Ca,L}$ = L-type calcium channel currents

SERCA2a = sarcoplasmic reticulum Ca^{2+}-ATPase

Adenosine monophosphate-activated protein kinase (AMPK), a serine/threonine kinase, is a sensor of cellular energy status and is expressed in many tissues and cell types, including cardiomyocytes (1,2). AMPK is composed of a catalytic α-subunit and regulatory β- and γ-subunits, forming a heterotrimer (1,2). With metabolic disturbance, AMPK is activated by phosphorylation in response to increased AMP/adenosine triphosphate (ATP) ratios; it modulates downstream signaling to compensate for energy depletion by increasing energy availability while decreasing energy expenditure (1,2). AMPK alleviates cellular dysfunction caused by conditions like left ventricular hypertrophy (3), heart failure (3), and ischemia (4). Cardiac electrophysiology may be regulated by AMPK, because substantial energy is required for the functional integrity of ion channels, transporters, and exchangers (1,2,5). However, the role of AMPK in cardiac electrophysiology is not fully understood, and almost nothing is known about its functional role in the atria.

SEE PAGE 59

The most common sustained clinical arrhythmia, atrial fibrillation (AF) produces a range of adverse health outcomes. AF causes atrial calcium ion (Ca^{2+})-handling abnormalities and hypocontractility, which are important in thrombus formation, therapeutic resistance, and stroke (6). Metabolomic and proteomic analyses indicate a close relationship between metabolic dysfunction and AF development (7), suggesting that AMPK might be activated under AF conditions in an attempt to compensate for metabolic dysfunction.

We undertook the present study to assess whether AMPK is activated in left atrial (LA) cardiomyocytes under metabolic stress conditions; whether AMPK regulates Ca^{2+} handling and contractile properties of LA cardiomyocytes; and whether AMPK is activated in experimental and clinical AF.

METHODS

ANIMAL AND HUMAN MODELS. LA cardiomyocytes from 51 mongrel dogs were isolated as described previously (8). After cells were isolated, they were kept in 200 μmol/l Ca^{2+}-containing Tyrode's solution for Ca^{2+} imaging experiments.

Neonatal rat ventricular cardiomyocytes (NRVM) were isolated using NRVM isolation system kits (Worthington Biochemical Corp., Lakewood, New Jersey) and cultured for small interfering RNA (siRNA)-based AMPK knockdown experiments.

All animal care and handling procedures followed National Institutes of Health guidelines and were approved by the Montreal Heart Institute Animals Research Ethics Committee. Eight mongrel dogs (20 kg to 36 kg) were divided into control and atrial-tachypacing groups. Dogs were anesthetized with ketamine (5.3 mg/kg, intravenous [IV])/diazepam (0.25 mg/kg, IV)/isoflurane (1.5%), intubated, and ventilated. A unipolar pacing lead was inserted into the right atrial (RA) appendage under fluoroscopic guidance and connected to a pacemaker in the neck. Bipolar electrodes were inserted into the right ventricular apex and RA appendage for electrogram recording. The pacemaker was programmed to stimulate the RA at 600 beats/min for 1 week with fibrillatory atrial activity during pacing confirmed by daily electrocardiographic and intracardiac recordings (9). On day 7, dogs were anesthetized with morphine (2 mg/kg subcutaneous [SC]) and α-chloralose (120 mg/kg IV, followed by 29.25 mg/kg/h) and ventilated. A median sternotomy was performed, and an LA-appendage sample was taken from the beating heart and immediately frozen in liquid nitrogen to avoid changes in cellular metabolic state.

RA appendages were obtained from 10 sinus rhythm (control) patients, 7 paroxysmal AF patients (pAF) (in whom the latest episode was >7 days preoperatively), and 9 patients with longstanding, persistent AF (cAF) (>6 months) (Online Table 1) who underwent open heart surgery for coronary artery and/or valvular heart disease. Appendages were snap frozen in liquid nitrogen for biochemical studies. Experimental protocols were approved by the ethics committee of the Universities of Heidelberg (2011-216N-MA) and Duisburg-Essen (12-5268-BO). Each patient gave written informed consent. Atrial cardiomyocytes were isolated from 4 control patients (Online Table 2) with enzymatic digestion under Ca^{2+}-free perfusion as described previously (10).

doctoral studentship. Dr. Dobrev is supported by European Network for Translational Research in Atrial Fibrillation (FP7-HEALTH-2010, proposal 260157), and the European-North American Atrial Fibrillation Research Alliance Fondation Leducq grant 07CVD03. All other authors have reported they have no relationships relevant to the contents of this paper to disclose.
Listen to this manuscript's audio summary by *JACC* Editor-in-Chief Dr. Valentin Fuster.

Manuscript received May 15, 2014; revised manuscript received April 5, 2015, accepted April 23, 2015.

Canine LA cardiomyocytes and siRNA-transfected NRVMs were incubated with Indo-1-AM (5 μmol/l) (Molecular Probes, Eugene, Oregon) in 100 μmol/l pluronic F-127 (Molecular Probes) and 0.5% dimethylsulfoxide (Sigma-Aldrich, St. Louis, Missouri) for ~5 min and then superfused with Tyrode's solution. For human cells, the fluorescent indicator fluo-3 acetoxymethyl (Fluo-3-AM) (Molecular Probes) was used as the fluorescent probe (10 μmol/l, 10-min loading, 30-min de-esterification). Fluorescence signal ratios were digitized and converted to intracellular calcium concentration ($[Ca^{2+}]_i$) as previously described (6,10,11). Cells were field stimulated by using 10-ms 1.5-threshold square-wave pulses at 36°C ± 1°C. CS was measured in canine LA cardiomyocyte with a video edge detector, with edge detection cursors positioned at both cell ends. All data were based on the average of 5 consecutive beats.

L-type Ca^{2+} current ($I_{Ca,L}$) was measured in canine LA cardiomyocytes and human atrial cardiomyocytes at 36°C ± 1°C in whole-cell ruptured-patch configuration, along with simultaneous measurement of corresponding triggered $[Ca^{2+}]_i$ transients, with a holding potential of −80 mV and a 100-ms ramp pulse to −40 mV to inactivate the fast Na^+ current, followed by a 100-ms test pulse to +10 mV at 0.5 Hz (10).

Caffeine-induced Ca^{2+} transients (CaTs) and corresponding sodium-calcium exchange (NCX) currents were simultaneously recorded in dog LA cardiomyocytes for quantification of sarcoplasmic reticulum (SR) Ca^{2+} content, as previously described (10). Membrane potential was held at −80 mV. SR Ca^{2+} content was assessed by rapidly applying caffeine (10 mmol/l) after 1 min of Ca^{2+} loading at 0.5 Hz with the $I_{Ca,L}$ voltage clamp protocol described above. Caffeine-induced NCX current was integrated to calculate SR Ca^{2+} content (10).

Freshly isolated LA cardiomyocytes from control dogs were plated onto laminin-coated (20 μg/ml) 4-well culture dishes and maintained at 37°C, 95% O_2/5% CO_2. After a 3-h incubation in culture medium (M-199 medium supplemented with 1% insulin-transferrin-selenium and 1% penicillin/streptomycin) (Life Technologies, Carlsbad, California), dead and unattached cardiomyocytes were removed, and fresh normal Tyrode's solution or glycolysis-inhibiting (GI) Tyrode's solution (with 10 mmol/l 2-deoxyglucose [Sigma-Aldrich] and 10 mmol/l sodium pyruvate [Sigma-Aldrich]; glucose-free) was added. Cells were maintained with or without field stimulation (square-wave 5-ms pulses) at 2 Hz for 20 min and were then fast frozen for subsequent biochemical study (studied in parallel for all experimental series) (12).

Protein samples were extracted, quantified, separated by 8% gel electrophoresis, and transferred to polyvinylidene-difluoride membranes. Sheep anti-rabbit immunoglobulin G (IgG) M-280-coated Dynabeads (Life Technologies) were used for immunoprecipitation. Isolated NRVMs were cultured to 60% to 80% confluence for siRNA transfection. Cells were maintained in culture until RNA extraction and quantitative polymerase chain reaction. BLOCK-iT Alexa Fluor red fluorescent control (Life Technologies) was used to confirm transfection efficiency.

ATP and AMP were quantified by high-performance liquid chromatography (HPLC). Analytical separation was performed using a MicroSpher C_{18} column (100 mm × 4.6 mm; internal diameter, 3 μm; Agilent Technologies, Santa Clara, California), and peak identities were confirmed by comparison of sample peak retention times with those of HPLC-grade nucleotide standards. Concentrations were calculated by comparing the peak area of samples with calibration curves of peak areas of standard compounds.

STATISTICAL ANALYSIS. All data are mean ± SEM. Two-way analysis of variance (ANOVA) with multiple group comparisons (Bonferroni-corrected Student *t* tests) was applied to data with 2 or more main effect factors. One-way ANOVA was applied for single main-effect-factor experiments. Repeated measures analyses were used when the same set of subjects or materials was exposed to multiple interventions. Student *t* tests were used for comparisons involving only 2 groups. For multiple comparisons with Bonferroni correction, adjusted p values were calculated by multiplying original p values by the number of comparisons (N) performed; values shown are adjusted values (N × p). A 2-tailed p value of <0.05 was considered statistically significant. Additional Methods details are described in the Online Appendix.

RESULTS

Figures 1A and 1B show representative recordings of CaT and CS under GI conditions. Diastolic $[Ca^{2+}]_i$ did not change with GI (**Figure 1C**). However, CaT amplitude and CS significantly decreased at 4 min and returned toward baseline at 8 min (**Figures 1D and 1E**), suggesting cellular adaptation to metabolic stress. Because AMPK activation might underlie cellular adaptation, we examined the effect of an AMPK inhibitor, compound C (CompC) (Sigma-Aldrich) at 10 μmol/l, on CaT and CS under metabolic stress. **Figures 1F and 1G** show representative recordings under GI conditions in the presence of CompC. AMPK blockade caused a large and progressive decrease in CaT and CS, with contractile

FIGURE 1 CaTs and CS After GI in Absence and Presence of Intact AMPK

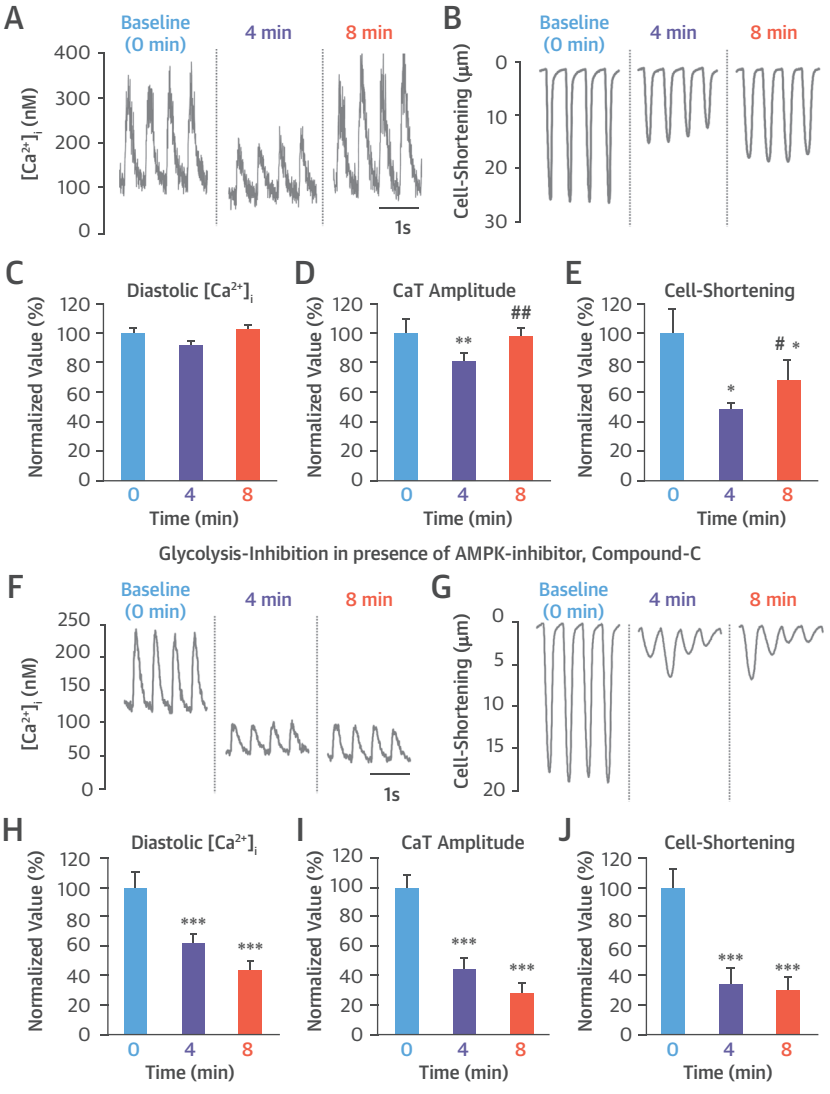

Recordings show **(A)** CaTs and **(B)** CS in atrial cardiomyocytes at 2 Hz as a function of time after GI. Diastolic $[Ca^{2+}]_i$ **(C)** (n = 13 dogs/19 cells), CaT amplitude **(D)** (n = 13 dogs/19 cells); and CS **(E)** (n = 4 dogs/7 cells) are normalized to baseline values at 0, 4, and 8 min (data are mean ± SEM). Recordings of CaTs **(F)** and CS **(G)** during GI in the presence of the AMPK inhibitor compound C (CompC; 10 μmol/l). Diastolic intracellular calcium concentration $[Ca^{2+}]_i$ **(H)** (n = 5 dogs/10 cells), CaT amplitude **(I)** (n = 5 dogs/10 cells), and CS **(J)** (n = 5 dogs/11 cells) decrease in the presence of compound C (data are mean ± SEM). *p < 0.01; **p < 0.001 vs. 0 min; ***p < 0.001 vs. baseline; #p < 0.05; ##p < 0.01 vs. 4 min. AMPK = adenosine monophosphate-regulated protein kinase; Ca^{2+} = calcium ion; CaTs = Ca^{2+} transients; $[Ca^{2+}]_i$ = intracellular calcium concentration; CS = cell shortening; GI = glycolysis inhibition.

function becoming destabilized in the presence of GI plus CompC (Figures 1H to 1J), suggesting that intact AMPK is essential for atrial cardiomyocyte adaptation to metabolic stress.

We next directly examined whether LA cardiomyocyte AMPK was activated (phosphorylated) by metabolic stress. Figure 2A shows immunoblots of phosphorylated AMPK, total AMPK, and GAPDH in nonpaced and 2-Hz-paced cells with and without GI. The phosphorylated AMPK/total AMPK ratio increased slightly with GI or 2-Hz pacing only but quite substantially with combined GI and 2-Hz pacing (Figure 2B). Because AMPK is activated in response to increased AMP/ATP ratio, we quantified cellular AMP and ATP by HPLC in GI-exposed and/or 2 Hz-paced or nonpaced cardiomyocytes. The AMP/ATP ratio

increased slightly with 2 Hz pacing compared with that under nonpaced conditions and increased further with the addition of GI (Online Figure 1).

AMPK EFFECTS. Results shown in **Figure 1** suggest that AMPK is important for maintaining cardiomyocyte Ca^{2+} stores, particularly under metabolic stress. We therefore directly evaluated the effect of blocking AMPK on SR Ca^{2+} content by simultaneously measuring caffeine-induced CaT and NCX currents. **Figure 3A** shows representative recordings in the absence or presence of CompC, respectively. AMPK blockade significantly decreased caffeine-induced NCX current amplitude and SR Ca^{2+} content (**Figure 3B**) without affecting $[Ca^{2+}]_i$ decay kinetics (**Figure 3C**).

We next tested whether the direct AMPK activator 5-aminoimidazole-4-carboxamide ribonucleotide (AICAR) (1 mmol/l) (Cell Signaling, Danvers, Massachusetts) affected Ca^{2+} handling and cell contraction. CaT and CS were measured in atrial cardiomyocytes paced at 2 Hz before and after 10-min AICAR incubation. **Figures 4A and 4B** show representative recordings. AMPK activation increased CaT amplitude amd CS but did not change diastolic $[Ca^{2+}]_i$ (**Figures 4C to 4E**). We then tested AICAR's ability to overcome the effects of AMPK inhibition on CaT and CS. Preincubation with AICAR partially prevented CompC-induced decreases in CaT amplitude and CS (**Figures 4F to 4J**) without affecting diastolic $[Ca^{2+}]_i$.

Voltage-gated L-type Ca^{2+} channels play a critical role in cardiomyocyte Ca^{2+} handling and excitation-contraction coupling (12–14) and have been reported

FIGURE 2 Effects of Metabolic Stress on AMPK Phosphorylation

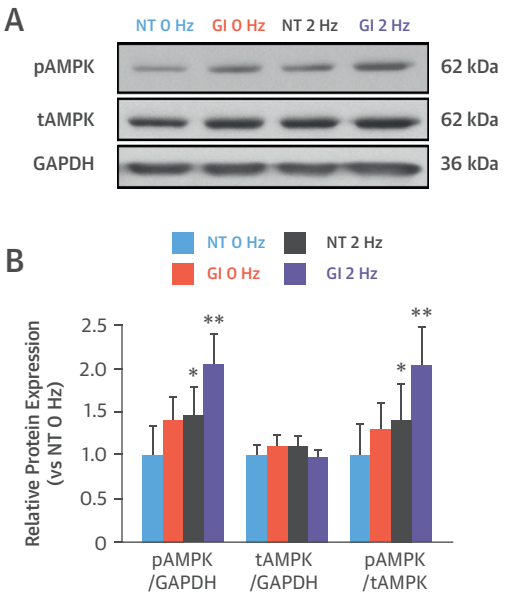

(A) Representative immunoblots for pAMPK, tAMPK, and GAPDH in atrial cardiomyocytes with or without 2-Hz stimulation in the presence or absence of GI. **(B)** pAMPK, tAMPK, and pAMPK/tAMPK ratio (all relative to GAPDH; n = 7 experiments/group) demonstrated various responses to GI and/or 2-Hz pacing. Data are mean ± SEM. *p < 0.05; **p < 0.01 vs. normal Tyrode solution (NT) without pacing. GAPDH = glyceraldehyde 3-phosphate dehydrogenase; pAMPK = phosphorylated AMPK; tAMPK = total AMPK; other abbreviations as in **Figure 1**.

FIGURE 3 Effects of AMPK Inhibition on $I_{Ca,L}$ Current and Cellular Ca^{2+} Handling

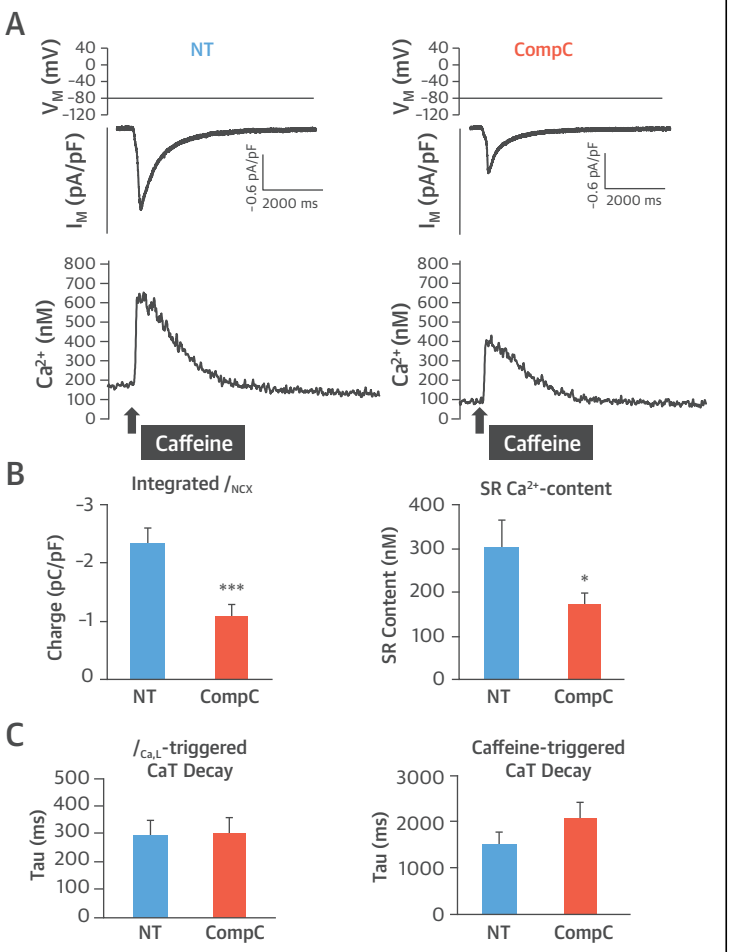

(A) Membrane currents (I_m) **(top)** and $[Ca^{2+}]_i$ **(bottom)** respond to caffeine (10 mmol/l) in NT **(left)** and in the presence of compound C (CompC) **(right)**. **(B)** Integrated membrane current carried by the Na^+/Ca^{2+} exchanger (NCX; mean ± SEM) in response to caffeine, which is used to estimate total sarcoplasmic reticulum (SR) Ca^{2+} content **(left)**; SR Ca^{2+} content (mean ± SEM; right). **(C)** Decay time constants (mean ± SEM) of CaT induced by $I_{Ca,L}$ **(left)** or caffeine **(right)**. n = 5 dogs/7 cells. *p < 0.05 and ***p < 0.001 vs. NT. $I_{Ca,L}$ = L-type calcium current; NT = normal Tyrode solution; other abbreviations as in **Figures 1 and 2**.

to depend on glycolytically derived ATP for functional integrity (15). Because AMPK activates the glycolysis pathway, we hypothesized that AMPK contributes to the functional regulation of L-type Ca^{2+} channels. We therefore simultaneously measured $I_{Ca,L}$ and $I_{Ca,L}$-induced CaTs in the presence or absence of CompC. **Figure 5A** shows representative recordings. AMPK inhibition decreased $I_{Ca,L}$ density, causing a parallel decrease in diastolic $[Ca^{2+}]_i$ and CaT amplitude (**Figures 5B to 5D**). We also measured $I_{Ca,L}$ and $I_{Ca,L}$-induced CaTs in atrial cardiomyocytes from sinus rhythm patients undergoing cardiac surgery. Patient characteristics are shown in Online Table 1; and Online Figure 2A shows representative recordings. CompC decreased $I_{Ca,L}$ density, diastolic $[Ca^{2+}]_i$, and CaT amplitude without affecting $[Ca^{2+}]_i$ decay kinetics (Online Figures 2B to 2D), similar to results in dog atrial cardiomyocytes. These data suggest that $I_{Ca,L}$ may be a

FIGURE 4 Effects of AMPK Activation on CaTs and CS

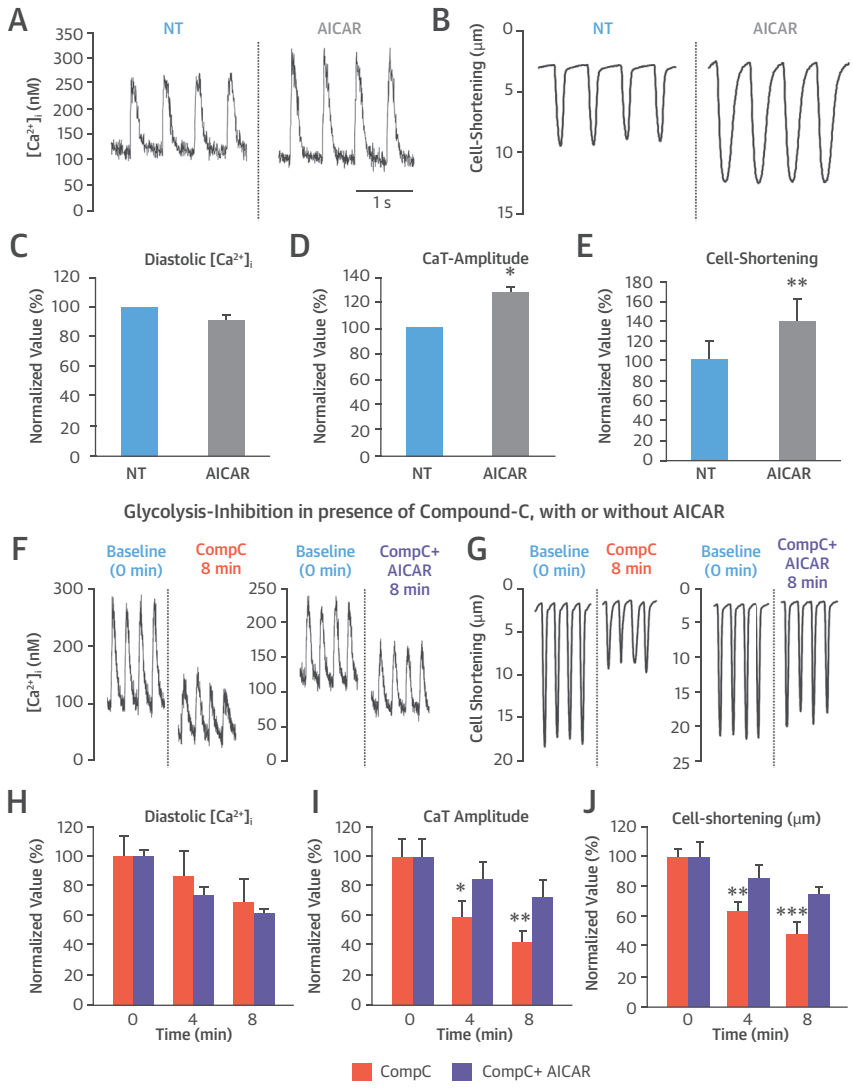

Recordings of CaTs **(A)** and CS **(B)** in atrial cardiomyocytes before and after an AMPK activator, 5-aminoimidazole-4-carboxamide ribonucleotide (AICAR; 1 mmol/l). AMPK activation did not affect diastolic $[Ca^{2+}]_i$ **(C)** (mean ± SEM; n = 4 dogs/6 cells) but did increase CaT amplitude **(D)** (mean ± SEM; n = 4 dogs/6 cells; *p < 0.05 vs. NT) CS **(E)** (mean ± SEM; n = 5 dogs/7 cells; **p < 0.01 vs. NT); all values were normalized to those of baseline. CaT **(F)** and CS **(G)** recordings in AMPK inhibitor with or without AMPK activator. Preincubation with AICAR did not affect $[Ca^{2+}]_i$ **(H)** (mean ± SEM; n = 6 dogs/7 cells) but partially prevented CompC-induced decreases in CaT amplitude **(I)** (mean ± SEM; n = 7 dogs/7 cells) and CS **(J)** (mean ± SEM; n = 7 dogs/7 cells; *p < 0.05; **p < 0.01; ***p < 0.001 vs. baseline).

primary target for AMPK regulation of cellular Ca^{2+} handling.

Recent evidence suggests that AMPK may directly activate downstream targets like ion channel subunits to regulate cell function (16). To examine whether AMPK interacts physically with Ca^{2+}-handling proteins, membrane-protein fractions from canine LA tissues were immunoprecipitated with AMPKα antibodies, and then immunoblotting was performed. RyR2, SERCA2a, and PLB did not immunoprecipitate with AMPK (Online Figures 3A to 3D). However, AMPK coimmunoprecipitated with $Ca_v1.2$ (**Figure 5E**), suggesting that AMPK either directly interacts with $I_{Ca,L}$ α-subunits or is colocalized along with $I_{Ca,L}$ α-subunits in a macromolecular complex. NCX1 also coimmunoprecipitated with AMPK (Online Figure 3E).

To confirm the effect of AMPK suppression, we performed siRNA-based AMPKα knockdown in NRVMs. AMPKα1 and AMPKα2 messenger expression levels decreased by >90% in AMPKα1- and AMPKα2-siRNA-transfected NRVMs, respectively (**Figures 6A and 6B**). **Figures 6C and 6D** show representative CaT recordings with or without AMPKα subunit knockdown. Also, siRNA-based AMPKα-knockdown decreased diastolic $[Ca^{2+}]_i$ and CaT amplitude (**Figures 6E and 6F**). These data confirm that AMPK is involved in the regulation of cardiomyocyte Ca^{2+} handling.

FIGURE 5 **Interactions Between AMPK and L-type Ca^{2+} Channels**

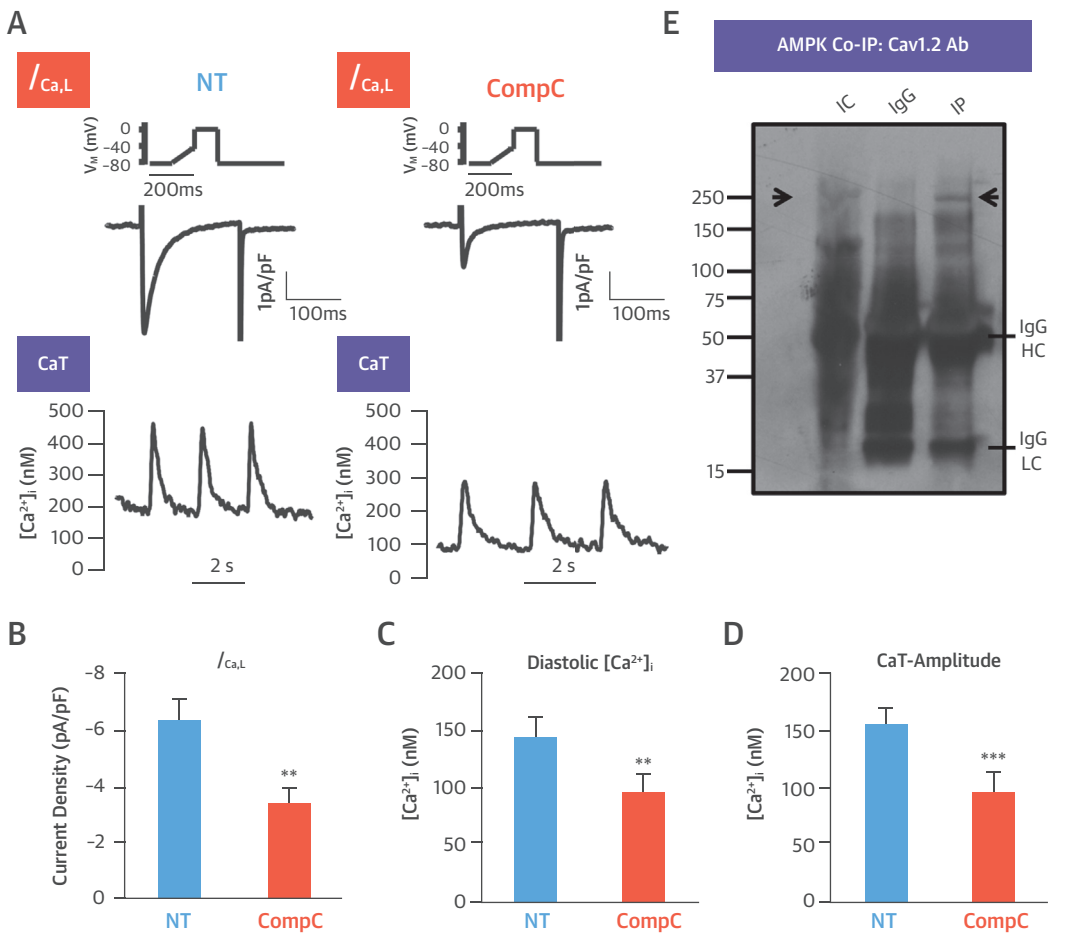

(A) Representative recordings of $I_{Ca,L}$-triggered CaTs in atrial cardiomyocytes of control dogs. Voltage clamp protocol **(top)** with recordings of $I_{Ca,L}$ **(middle)** and CaT **(bottom)** in the absence (NT **[left]**) or presence **(right)** of CompC (10 μmol/l). AMPK inhibition decreased **(B)** $I_{Ca,L}$, **(C)** diastolic $[Ca^{2+}]_i$, and **(D)** CaT (data are mean ± SEM; n = 6 dogs/10 cells; **p < 0.01 and ***p < 0.001 vs. NT). **(E)** Membrane fractions of canine atrial cardiomyocytes were immunoprecipitated with anti-AMPK antibody, and Western blotting was performed with antibody (Ab) directed against calcium channel, voltage-dependent, L-type, alpha 1C subunit ($Ca_v1.2$). IC = input control; IgG = nonimmune rabbit immunoglobulin G (IgG) (negative control); IP = immunoprecipitation; other abbreviations as in **Figures 1 and 3**.

FIGURE 6 Effects of AMPK Knockdown on Ca^{2+} Handling

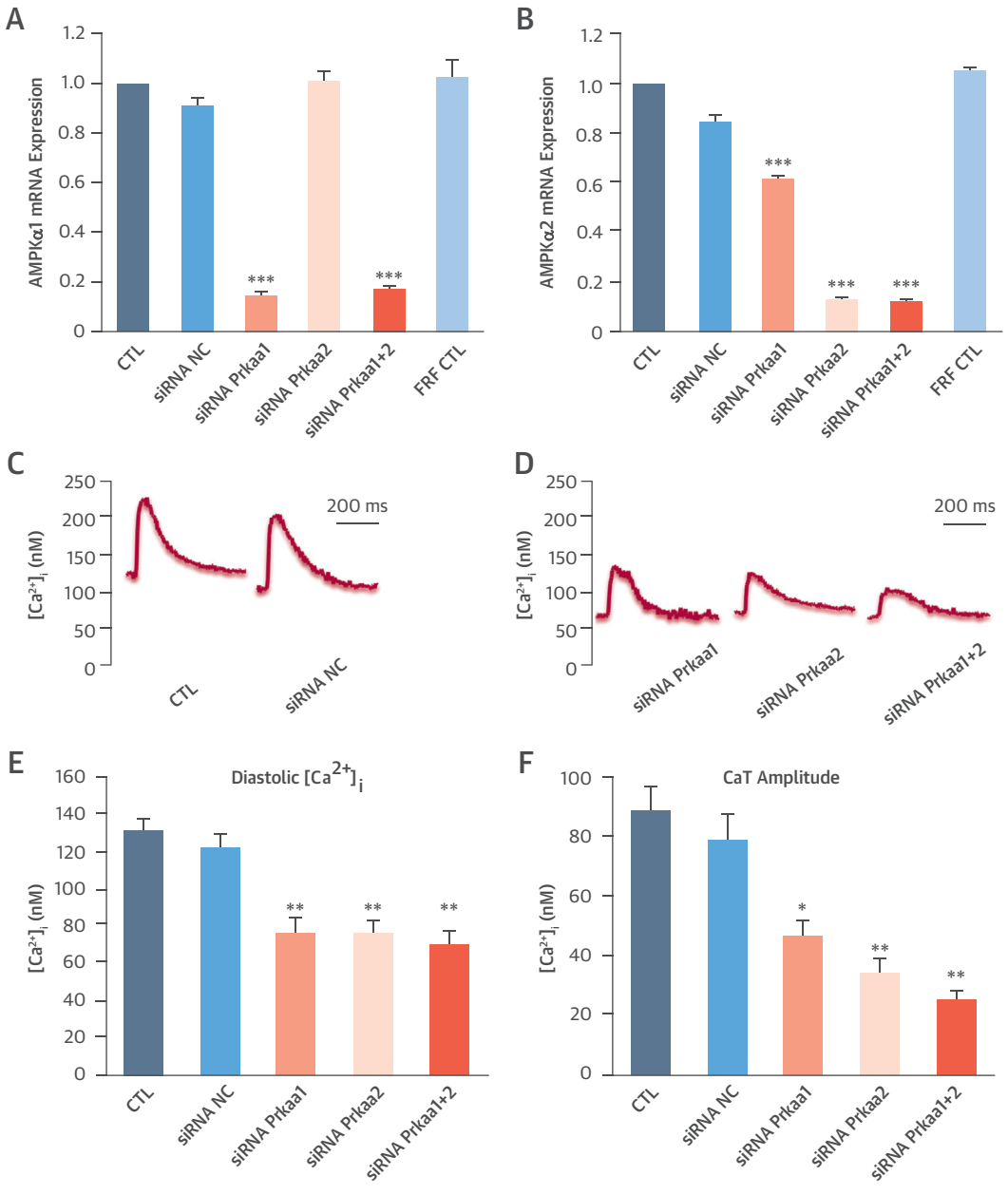

(A) Relative mRNA expression of AMPKα1 in neonatal rat ventricular cardiomyocytes (NRVMs) transfected with AMPKα1-siRNA (Prkaa1), AMPKα2-siRNA (Prkaa2), and negative control-siRNA (NC). FRF control: Alexa Fluor-red fluorescent control. Data are mean ± SEM (relative to nontransfection control [CTL]; n = 5 independent experiments/group). **(B)** Relative AMPKα2 mRNA-expression (n = 5/group). Representative CaT recordings **(C)** at 1 Hz in CTL and NC and **(D)** in Prkaa1, Prkaa2, and PrKaa1+2. **(E)** Mean ± SEM diastolic $[Ca^{2+}]_i$ (n = 5/group). **(F)** Mean ± SEM CaT amplitude (n = 5/group; *p < 0.05; **p < 0.01; ***p < 0.001 vs. NC). siRNA = small interfering ribonucleic acid.

AMPK ACTIVATION IN AF. AF is known to cause atrial Ca^{2+}-handling abnormalities and hypocontractility (6,10,13,14). There are clear metabolic disturbances in atrial tissue samples from AF patients (7). The rapid atrial rate in AF and associated increased cellular energy demand might induce an increase in the AMP/ATP ratio, activating AMPK. We therefore quantified AMPK phosphorylation in LA tissues from dogs maintained electrically in AF for 1 week. Figure 7A shows representative immunoblots for phosphorylated

(Thr172) AMPK, total AMPK, and GAPDH. AF significantly increased the phosphorylated AMPK/total AMPK ratio, indicating AMPK activation (**Figure 7B**).

We also evaluated the expression and phosphorylation of AMPK in AF patients. RA appendage tissues were obtained from sinus rhythm, pAF, and cAF patients undergoing cardiac surgery. Patient characteristics are shown in Online Table 2. Fractional AMPK phosphorylation at the Thr172 site was increased by ~50% in pAF patients (Online Figure 4A). In contrast, cAF patients showed a significant decrease in fractional AMPK phosphorylation (Online Figure 4B). However, absolute AMPK phosphorylation was not significantly affected in either group.

FIGURE 7 AMPK Activation by 1 Week of AF (Dog Model)

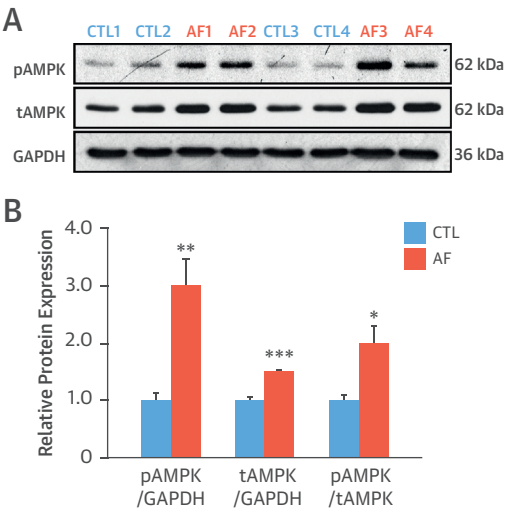

(A) Representative immunoblots for pAMPK, tAMPK, and GAPDH in left atrial tissues freshly obtained from control and electrically maintained atrial fibrillation (AF) dogs. **(B)** AF significantly increased pAMPK, tAMPK, and the pAMPK/tAMPK ratio (all relative to control [CTL]; n = 4/group; *p < 0.05; **p < 0.01; and ***p < 0.001 vs. control). Abbreviations as in **Figure 2**.

DISCUSSION

In the present study, we provide evidence for an important role of AMPK in regulating LA cardiomyocyte Ca^{2+} handling and contractility, particularly in response to metabolic stress. Furthermore, our data indicate that the functional integrity of $I_{Ca,L}$ requires intact AMPK activity and that AMPK interacts physically with the L-type Ca^{2+} channel α-subunit. We also demonstrate that AMPK is activated in experimental AF. Taken together, our results indicate that AMPK operates as a metabolic adaptor to protect the atria against the profibrillatory, and possibly prothrombotic, consequences resulting from AF-induced metabolic stress (**Central Illustration**).

COMPARISON WITH PREVIOUS STUDIES OF CARDIAC AMPK. Metabolic disturbances and associated electromechanical coupling abnormalities play a significant pathophysiological role in many cardiac disease processes. AMPK is activated by cellular energy depletion and compensates for metabolic abnormalities by increasing energy generation, and decreasing energy consumption (1,2). AMPK phosphorylation is a key activating signal (1,2). Although cardiac electrophysiology is closely linked to metabolic function, relatively little is known about the control of cardiac electrical activity by AMPK (2).

Several lines of evidence indicate that AMPK regulates cardiac contractility. Oliveira et al. (17) demonstrated that cardiac troponin I (cTnI) is a substrate for the AMPKγ2 subunit in mouse left ventricular cardiomyocytes. The phosphorylation of cTnI at Ser150 by the activated AMPK holoenzyme α1/β1/γ2 subunit complex increases myofilament Ca^{2+} sensitivity and augments contractility in vitro. The kinase domain of AMPK is sufficient to phosphorylate cTnI at Ser150 in the myofilament lattice (18). Nixon et al. (19) demonstrated that the physiologically relevant AMPK complex (α1/β1/γ2 subunit) phosphorylates cTnI at Ser150 in vitro within the myofilament lattice.

We demonstrated that pharmacological phosphorylation of the AMPKα subunit with AICAR increases contractility in dog atrial cardiomyocytes, an effect at least partially attributable to an AMPK-dependent increase in CaT amplitude. Oliveira et al. (17) also reported that AMPK phosphorylation increases contractility without changing CaT amplitude in mouse ventricular cardiomyocytes. This discrepancy might be due to differences in species (mouse vs. dog) and chambers (ventricle vs. atrium) studied. Even though CaT amplitude was unchanged, CaT decay kinetics slowed upon AMPKα phosphorylation in the study by Oliveira et al. (17), suggesting AMPK effects on Ca^{2+} handling.

Kockskamper et al. (20) examined the effect of intermediates and products of glycolysis on Ca^{2+} handling in ferret atrial cardiomyocytes. GI increased diastolic $[Ca^{2+}]_i$ and induced CaT alternans, followed by decreased CaT amplitude, consistent with our results. In this study, each intermediate and end product of glycolysis had a different impact on cellular Ca^{2+} handling. Of note, fructose-1,6-bisphosphate, a glycolysis intermediate regulated by phosphofructokinase-2, tremendously increased

CENTRAL ILLUSTRATION AMPK, Atrial Ca^{2+} Handling, and Atrial Fibrillation

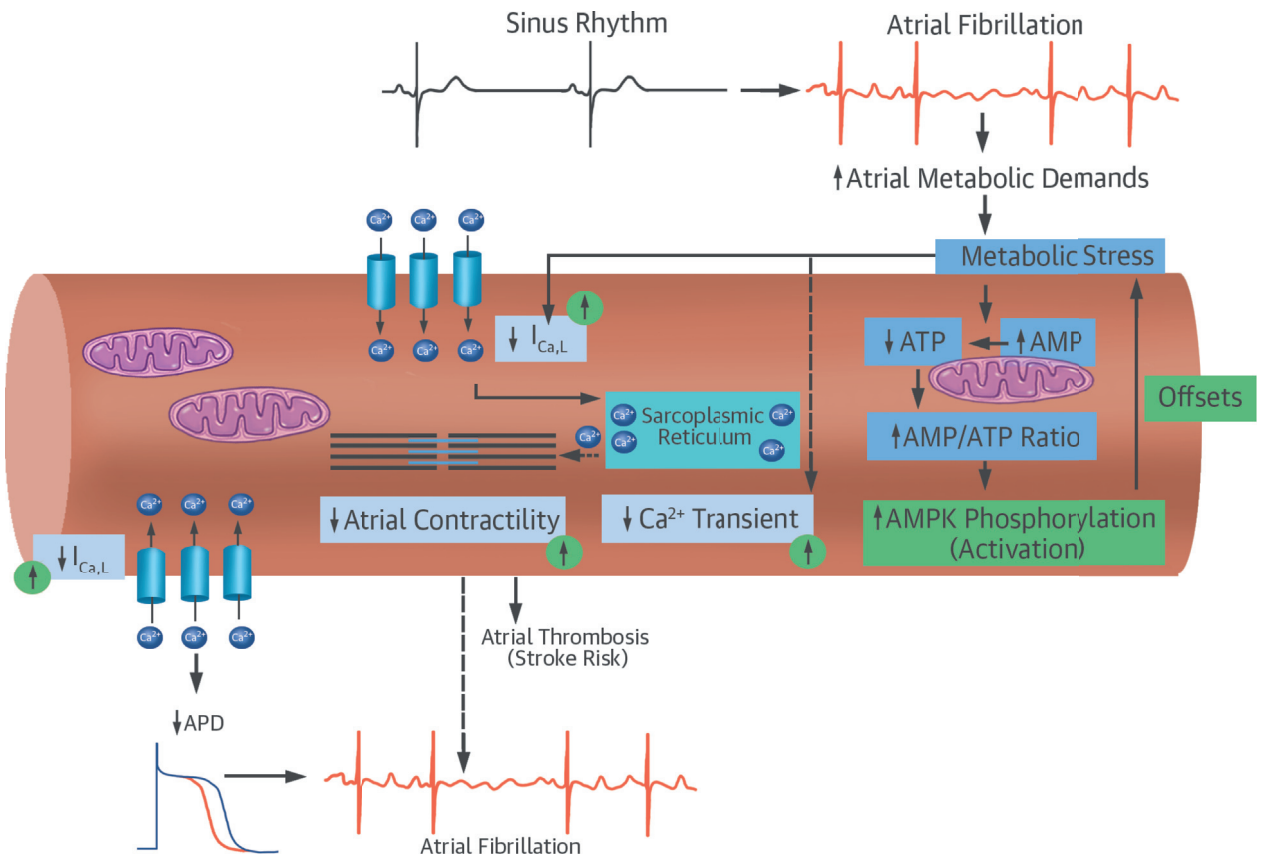

Harada, M. et al. J Am Coll Cardiol. 2015; 66(1):47–58.

Aspects we studied directly are **boxed**. Atrial fibrillation (AF) increases atrial rate, enhancing metabolic demands and inducing metabolic stress. Metabolic stress reduces $I_{Ca,L}$. Decreased $I_{Ca,L}$ reduces sarcoplasmic reticulum Ca^{2+}-stores, thus reducing the systolic Ca^{2+} transient. Decreased $I_{Ca,L}$ will also reduce APD, promoting AF, whereas decreased Ca^{2+} transients lead to reduced atrial contractility and thereby enhance thrombosis/stroke risk. Metabolic stress interferes with the ability of mitochondrial respiration to keep up with the enhanced need for ATP, causing an increase in the AMP/ATP ratio. The AMP/ATP ratio is the main factor regulating enzymes that phosphorylate AMPK; that is, when the ratio rises (indicating metabolic stress), AMPK phosphorylation is increased, activating AMPK. The AMPK activation resulting from AF-related metabolic stress in turn causes phosphorylation of a host of intracellular targets to reduce energy needs and enhance energy availability, which compensate the metabolic state. The AMPK-induced metabolic compensation offsets the reductions in $I_{Ca,L}$, Ca^{2+} transients, and atrial contractility caused by metabolic stress. Thus, AMPK is an important contributor to maintaining atrial functional integrity in the face of AF-induced metabolic stress. AMPK = adenosine monophosphate-regulated protein kinase; APD = action-potential duration; Ca^{2+} = calcium ion; $I_{Ca,L}$ = L-type calcium current.

open probability of ryanodine receptors (20). Because AMPK regulates phosphofructokinase-2 activity, AMPK activation would be expected to augment SR Ca^{2+} release through this mechanism.

We demonstrated that pharmacological AMPK modulation alters L-type Ca^{2+} channel function. ATP derived from glycolysis is preferentially used for regulation of $I_{Ca,L}$ (15). Glycolytic enzymes colocalize with skeletal muscle Ca^{2+} channels (21). AMPK activation increases glycolytic ATP and/or potentially conserves ATP by turning off anabolic pathways, which may increase energy available for L-type Ca^{2+} channel regulation. AMPK inhibits the ion-channel activity of BK_{Ca} (22) and Kir6.2 (23,24) by direct phosphorylation, whereas it increases the activity of Kv2.1 (16). In the present study, AMPK was found to both regulate $I_{Ca,L}$ function and physically associate with $Ca_v1.2$ channel subunits. Thus, direct modulation of ion-channel function is an additional potential pathway for AMPK action in this system. $Ca_v1.2$ channel activity is known to be regulated by various protein kinases/phosphatases including PKA, PKC, and PP1 (25,26), but to our knowledge, AMPK regulation of $Ca_v1.2$ has not previously been reported.

POTENTIAL MECHANISMS, NOVELTY, AND SIGNIFICANCE. The orchestration of ion channels, transporters, and exchangers requires substantial energy; therefore, pathological metabolic stress could dysregulate cellular electrophysiology. AF is associated with important metabolic abnormalities (7), and cellular energetic state is closely related to the ability to sustain AF in dogs with tachycardiomyopathic heart failure (27). AMPK is activated to compensate for energy depletion by accelerating glycolysis and fatty-acid oxidation (1,2). In the present study, AMPK was hyperphosphorylated in the canine LA by acute metabolic stress and by 1 week of electrically maintained AF. Combined with our studies of Ca^{2+} handling, these results point to a potentially important compensatory role of AMPK in AF. Ikeda et al. (28) demonstrated the importance of AMPK in maintaining cardiac function (28). Knockout of LKB1, an AMPK kinase implicated in AMPK activation, decreased AMPK activity and impaired cardiac contractility in association with reduced PLB and SERCA2a expression. Of note, the effect of LKB1 knockout was much greater in atrium than in ventricle, and knockout mice showed substantial atrial remodeling along with spontaneous AF (28).

We provide evidence showing that AMPK fractional phosphorylation is increased in pAF patients and decreased in cAF patients. It may be that enhanced AMPK activity helps to protect pAF patients from arrhythmia persistence, whereas failure of AMPK phosphorylation may contribute to the chronicity and therapeutic resistance that characterizes long-term AF. AMPK activity is reduced with age, potentially contributing to decreased stress tolerance in the elderly population (29); AF vulnerability increases with aging (6). Macrophage migration inhibitory factor (MIF) modulates AMPK activation, and genetic variability in MIF expression may affect AMPK pathway responsiveness (29). Thus, MIF variability is a candidate mechanism to explain AMPK variability and any potential contribution to AF chronicity.

Progression of AF to increasingly persistent forms is a major clinical challenge (30). The overall progression rate from paroxysmal to persistent AF is approximately 5% per year (30). The factors determining which patients will progress are poorly understood, and better therapeutic approaches to prevent progression are needed (30). The present study raises the interesting possibilities that AMPK activation might contribute to resistance to AF progression and that therapeutic modulation of AMPK might be useful to prevent AF progression and improve therapeutic tractability.

STUDY LIMITATIONS. We used pharmacological tools to modulate AMPK and to examine its acute effect on cellular electrophysiology. However, all pharmacological probes, especially kinase inhibitors such as CompC, are imperfectly specific, and we cannot exclude the possibility of off-target effects.

Cellular metabolic state can be altered during cell isolation and no in vitro system completely reproduces the complex in vivo milieu; therefore, our results need to be interpreted cautiously. Additionally, the metabolic disturbances in clinical AF are much more complicated than the simple in vitro model we used here and occur on a complex remodeling background.

We provide evidence showing that AMPK phosphorylation fraction increases in pAF patients and decreases in cAF patients; however, absolute AMPK phosphorylation did not change, and we were unable to show hyperphosphorylation of AMPK targets. Also, although we showed an increase in the AMP/ATP ratio and increased AMPK phosphorylation with metabolic stress, we did not directly measure AMPK activity. Further work will be necessary to clarify the state of AMPK phosphorylation, as well as the relevant targets, at different phases of AF. Additional studies of the role of atrial metabolic dysfunction in general, and of AMPK in particular, in both experimental and clinical AF models are needed to probe this important and underexplored area.

We identified $I_{Ca,L}$ as an important mediator of AMPK effects on Ca^{2+} handling and cell contractility. However, participation of other components is not excluded; indeed, the instability of cell shortening combined with GI and AMPK inhibition suggests the contribution of other energy-dependent mechanisms. Further work will be required to detail all the mechanisms by which AMPK contributes to the adaptation of atrial cardiomyocytes to metabolic stress.

CONCLUSIONS

AF-associated metabolic stress impairs atrial Ca^{2+} handling and contractility, but also activates AMPK, which offsets these deleterious effects. AMPK may be an interesting new therapeutic target in AF.

ACKNOWLEDGMENTS The authors thank Nathalie L'Heureux, Chantal St-Cyr, Ramona Nagel, and Kathrin Kupser for technical help and France Thériault for secretarial assistance.

REPRINT REQUESTS AND CORRESPONDENCE: Dr. Stanley Nattel, Montreal Heart Institute, 5000 Belanger Street East, Montreal, Quebec H1T 1C8, Canada. E-mail: stanley.nattel@icm-mhi.org.

PERSPECTIVES

COMPETENCY IN MEDICAL KNOWLEDGE: AMPK contributes to the cellular adaptation to metabolic stress that has been implicated in the inception and maintenance of AF.

TRANSLATIONAL OUTLOOK: Future studies should examine the therapeutic impact of interventions such as AMPK activation that reduce metabolic stress to prevent progression of the substrate underlying the perpetuation of AF.

REFERENCES

1. Arad M, Seidman CE, Seidman JG. AMP-activated protein kinase in the heart: role during health and disease. Circ Res 2007;100:474–88.

2. Harada M, Nattel SN, Nattel S. AMP-activated protein kinase potential role in cardiac electrophysiology and arrhythmia. Circ Arrhythm Electrophysiol 2012;5:860–7.

3. Beauloye C, Bertrand L, Horman S, Hue L. AMPK activation, a preventive therapeutic target in the transition from cardiac injury to heart failure. Cardiovasc Res 2011;90:224–33.

4. Young LH. AMP-activated protein kinase conducts the ischemic stress response orchestra. Circulation 2008;117:832–40.

5. Barth AS, Tomaselli GF. Cardiac metabolism and arrhythmias. Circ Arrhythm Electrophysiol 2009;2:327–35.

6. Wakili R, Yeh YH, Qi XY, et al. Multiple potential molecular contributions to atrial hypocontractility caused by atrial tachycardia remodeling in dogs. Circ Arrhythm Electrophysiol 2010;3:530–41.

7. Mayr M, Yusuf S, Weir G, et al. Combined metabolomic and proteomic analysis of human atrial fibrillation. J Am Col Cardiol 2008;51:585–94.

8. Qi XY, Yeh YH, Xiao L, et al. Cellular signaling underlying atrial tachycardia remodeling of L-type calcium current. Circ Res 2008;103:845–54.

9. Harada M, Luo X, Qi XY, et al. Transient receptor potential canonical-3 channel-dependent fibroblast regulation in atrial fibrillation. Circulation 2012;126:2051–64.

10. Voigt N, Li N, Wang Q, et al. Enhanced sarcoplasmic reticulum Ca^{2+} leak and increased Na^{+}-Ca^{2+} exchanger function underlie delayed after depolarizations in patients with chronic atrial fibrillation. Circulation 2012;125:2059–70.

11. Nishida K, Qi XY, Wakili R, et al. Mechanisms of atrial tachyarrhythmias associated with coronary artery occlusion in a chronic canine model. Circulation 2011;123:137–46.

12. Makary S, Voigt N, Maguy A, et al. Differential protein kinase C isoform regulation and increased constitutive activity of acetylcholine-regulated potassium channels in atrial remodeling. Circ Res 2011;109:1031–43.

13. Voigt N, Heijman J, Wang Q, et al. Cellular and molecular mechanisms of atrial arrhythmogenesis in patients with paroxysmal atrial fibrillation. Circulation 2014;129:145–56.

14. Greiser M, Lederer WJ, Schotten U. Alterations of atrial Ca^{2+} handling as cause and consequence of atrial fibrillation. Cardiovasc Res 2011;89:722–33.

15. Losito VA, Tsushima RG, Diaz RJ, Wilson GJ, Backx PH. Preferential regulation of rabbit cardiac L-type Ca^{2+} current by glycolytic derived ATP via a direct allosteric pathway. J Physiol 1998;511:67–78.

16. Ikematus N, Dallas ML, Ross FA, et al. Phosphorylation of the voltage-gated potassium channel Kv2.1 by AMP-activated protein kinase regulates membrane excitability. Proc Natl Acad Sci U S A 2011;108:18132–7.

17. Oliveria SM, Zhang YH, Solis RS, et al. AMP-activated protein kinase phosphorylates cardiac troponin I and alters contractility of murine ventricular myocytes. Circ Res 2012;110:1192–201.

18. Sancho Solis R, Ge Y, Walker JW. A preferred AMPK phosphorylation site adjacent to the inhibitory loop of cardiac and skeletal troponin I. Protein Sci 2011;20:894–907.

19. Nixon BR, Thawornkaiwong A, Jin J, et al. AMP-activated protein kinase phosphorylates cardiac troponin I at Ser-150 to increase myofilament calcium sensitivity and blunt PKA-dependent function. J Biol Chem 2012;287:19136–47.

20. Kockskamper J, Zima AV, Blatter LA. Modulation of sarcoplasmic reticulum Ca^{2+} release by glycolysis in cat atrial myocytes. J Physiol 2005;564:697–714.

21. Brandt NR, Caswell AH, Wen SR, Talvenheimo JA. Molecular interaction of the junctional foot protein and dihydropyridine receptor in skeletal muscle triads. J Membr Biol 1990;13:237–51.

22. Wyatt CN, Mustard KJ, Pearson SA, et al. AMP-activated protein kinase mediates carotid body excitation by hypoxia. J Biol Chem 2007;282:8092–8.

23. Chang TJ, Chen WP, Yang C, et al. Serine-385 phosphorylation of inwardly rectifying K^{+} channel subunit (Kir6.2) by AMP-dependent protein kinase plays a key role in rosiglitazone-induced closure of the K(ATP) channel and insulin secretion in rats. Diabetologia 2009;52:1112–21.

24. Turrell HE, Rodrigo GC, Norman RI, Dickens M, Standen NB. Phenylephrine preconditioning involves modulation of cardiac sarcolemmal ATP-sensitive K^{+} current by PKC delta, AMPK and p38 MAPK. J Mol Cell Cardiol 2011;51:370–80.

25. Harvey RD, Hell JW. Cav1.2 signaling complexes in the heart. J Mol Cell Cardiol 2013;58:143–52.

26. Bodi I, Mikala G, Koch SE, Akhter SA, Schwartz A. The L-type calcium channel in the heart: the beat goes on. J Clin Invest 2005;115:3306–17.

27. Cha YM, Dzeja PP, Shen WK, et al. Failing atrial myocardium: energetic deficits accompany structural remodeling and electrical instability. Am J Physiol Heart Circ Physiol 2003;284:H1313–20.

28. Ikeda Y, Sato K, Pimentel DR, et al. Cardiac-specific deletion of LKB1 leads to hypertrophy and dysfunction. J Biol Chem 2009;284:35839–49.

29. Ma H, Wang J, Thomas P, et al. Impaired macrophage migration inhibitory factor-AMP activated protein kinase activation and ischemic recovery in the senescent heart. Circulation 2010;122:282–92.

30. Nattel S, Guasch E, Savelieva I, et al. Early management of atrial fibrillation to prevent cardiovascular complications. Eur Heart J 2014;35:1448–56.

KEY WORDS cell calcium handling, heart pharmacology, myocardial energy metabolism

APPENDIX For an expanded Methods section and supplemental figures and tables, please see the online version of this article.